Statistical kinetic approach to nuclear liquid-gas phase transition

Larissa V. Bravina and Eugene E. Zabrodin
Department of Physics, University of Bergen, Allègaten 55, N-5007 Bergen, Norway
and Institute for Nuclear Physics, Moscow State University, 119899 Moscow, Russia
(Received 17 April 1996)

Statistic approach based on the kinetics of a first-order phase transition is proposed for the description of multifragmentation phenomenon. We start from the thermalized gaslike system of nucleons and calculate the fragmentation yields according to classical nucleation theory. The fragmentation distributions are derived from the steady-state solution of a Fokker-Planck equation for the distribution function. Curvature energy and Coulomb energy in the form provided by the Wigner-Seitz approximation are included into the fragment formation energy. The fit to experimental data is performed. It is shown that the Coulomb interaction may lead to the deviation of the fragmentation yields from the power-law dependence. This prediction may be verified experimentally in heavy-ion central collisions at the energies about 40*A* MeV. [S0556-2813(96)00111-2]

PACS number(s): 25.70.Pq, 05.70.Fh, 21.10.Sf, 21.65.+f

I. INTRODUCTION

Although the search for the quark-hadron phase transition remains the most attractive goal of the experiments planned in high energy physics, the liquid-gas phase transition in nuclear matter at intermediate energies still represents a challenge for both experimentalists and theoreticians. The power-law falloff of the fragment mass distribution in proton induced reactions observed by the Purdue-Fermilab Collaboration [1] inspired the interest to macroscopic models based on the Fisher theory of condensation [2]. The possibility of the liquid-gas phase transition in a thermally equilibrated nuclear matter and applicability of the nucleation theory to nuclear reactions were discussed in many papers (see, e.g., [3–7], and references therein).

Since more and more experimental results have been available for the analysis, their interpretation as a critical phenomenon has been revised. It was mentioned in [4–6] that, in spite of the characteristic power-law dependence of the fragment mass distribution, different nuclear systems with different excitation energies cannot hit the critical point accidentally. Therefore, the expanding hot fireball may be quenched into the metastable or unstable regions of nuclear matter where the phase transition of first order should take place. When the density of the system is low enough, say, 0.3 or 0.5 of the normal nuclear density ρ_0, the system breaks into the fragments. Thus, the fragment distribution should contain the information about the disintegration temperature of the system. The problem of calculating the fragment distribution corresponding to given temperature and density of the system plays an essential role for the data analysis.

With a purely thermodynamic approach, the probability for cluster formation of size A is given by

$$Y(A) = Y_0 A^{-\tau} \exp(aA - bA^{2/3}), \tag{1}$$

containing the bulk and surface free energies a and b, and critical exponent τ connected with the curvature energy [2]. A fit of the fragment size distributions with expression (1) is used to determine the critical temperature of the system at which surface tension vanishes [8], and the fragment distribution is purely determined by the power law $A^{-\tau}$.

This approach has a serious drawback. Namely, it is based heavily on the thermodynamic theory which is limited to the stage before the actual phase transition [9]. To treat the problem correctly one has to perform a kinetic analysis for the development of clusters of the new phase. One of the possible solutions is proposed in [10] where the bulk, surface, and curvature (or Fisher) terms are presented in the formation energy of nuclear clusters. The kinetic approach predicts the falloff for light fragments (which may be approximated by a simple power law) together with a kind of plateau for the yield of heavy fragments. On the other hand, it is not obvious that the fragment distribution would be the same after the Coulomb energy is taken into account. The main aim of the present paper is to verify how the inclusion of the Coulomb energy affects the behavior of the distribution function of clusters.

This paper is organized as follows. In Sec. II we derive the nucleation rates for the fragments of different sizes (masses). Coulomb and Fisher terms are taken into account in the formation energy of clusters. The clusterization Coulomb energy is calculated within the Wigner-Seitz approximation which is described in details in [11]. The expressions derived for the cluster distributions are used in Sec. III to fit the fragment charge distributions observed in experiments. The results are discussed in Conclusions.

II. THEORY OF A FIRST-ORDER PHASE TRANSITION

We will keep the aforementioned scenario of a fireball evolution as a working hypothesis. Modification does concern the stage of a gas-liquid phase transition, where the kinetics of cluster evolution comes into play. Our analysis is based on the classical nucleation theory developed for the first-order phase transition processes by Becker and Döring [12], and Zeldovich [13]. For the sake of simplicity the assumptions concerning the first-order phase transition can be stated in this way: (i) creation of the spherical clusters of new phase within the initially homogeneous medium is considered; (ii) the evaporation-condensation process is the

mechanism by which the clusters of the new phase lose or gain particles. This is one of the possible realizations of the Markov process [14]. In contrast to the nuclear fragmentation model with the binary scheme of cluster fusion and splitting [15], the classical nucleation theory assumes that an arbitrary cluster changes its size due to the attachment to it (or the loss by it) of the smallest single-particle cluster [9]. (iii) The characteristic time of the evaporation-condensation process is much less than the lifetime of the metastable state, $\tau_{\rm ev} \ll \tau_{\rm relax}$.

Practically all microscopic models like the Copenhagen model [11], Berlin model [16], GEMINI model [17], as well as BUU calculations [18] assume a time delay of about 100–200 fm/c that is required for the fragmentation of an expanded nuclear system.

(iv) No effects connected with the finite size of the system are taken into account.

A. Equilibrium distributions

According to the thermodynamic theory of fluctuations the equilibrium distribution of clusters of the new phase $f_0(R)$ is given by the Boltzmann distribution

$$f_0(R) = I_0 \exp\left(- \frac{\Delta F(R)}{T} \right), \tag{2}$$

where $\Delta F(R)$ is the free energy associated with the formation of cluster of size R, and I_0 is a preexponential factor. The above relation can be written in the following form

$$f_0(R) = I_0 \exp\left\{ \left[\frac{4\pi}{3} R^3 \Delta p - 4\pi R^2 \sigma - \tau T \ \ln A - \frac{3}{5} \frac{Z^2 e^2}{R} \left(1 - \frac{R}{R_{\rm cell}} \right) \right] \frac{1}{T} \right\} \tag{3}$$

containing the bulk, surface, curvature (or Fisher), and Coulomb terms in the formation energy. The exponent represents the Myers-Swiatecki formula for a spherical nucleus [19] generalized to the case of nonzero temperature. If the Coulomb energy is neglected the equilibrium distribution of fragments would be the same as given by Eq. (1). Here Δp is the difference between the pressure inside and outside the cluster, σ is the surface tension, A is the mass number, and Z is the charge of the cluster of radius $R = r_0 A^{1/3}$, r_0 is the baryon radius, and $R_{\rm cell}$ is the radius of the cell on which the cluster is embedded. It is implied in the Wigner-Seitz approximation that the whole volume of the system consists of the individual noninteracting cells containing one cluster in the center. Therefore, to calculate the change in the Coulomb energy due to the cluster formation one has to subtract the background Coulomb energy of the uniformly charged sphere of radius $R_{\rm cell}$ from the Coulomb energy of the charged cluster. Since the Coulomb energy of the uniformly charged sphere of radius R and charge Z is $(3/5)(Z^2 e^2/R)$, the extra Coulomb energy of an individual cell has the form given by Eq. (3). In terms of the baryon density inside the cluster ρ_L and average baryon density of the system ρ the ratio $R/R_{\rm cell}$ may be written as [11]

$$\frac{R}{R_{\rm cell}} = \left[\frac{(Z_0/A_0)\rho}{(Z/A)\rho_L} \right]^{1/3}, \tag{4}$$

where A_0 and Z_0 are the total mass number and the total charge of the system, respectively. We will use the empirical formula [20] connecting charge number Z to mass number A,

$$Z = \frac{A}{1.98 + 0.015 A^{2/3}}, \tag{5}$$

in our further calculations. It is convenient to define the equilibrium distribution function for clusters of arbitrary sizes $f_0(R)$ via the equilibrium distribution function for clusters of critical size $f_0(R_c)$:

$$f_0(R) = f_0(R_c) \exp\left[- \frac{\Delta F(R) - \Delta F(R_c)}{T} \right], \tag{6}$$

$$f_0(R_c) = I_0 \exp\left[- \frac{\Delta F(R_c)}{T} \right]. \tag{7}$$

The critical radius R_c can be found from the relation

$$\frac{\partial [\Delta F(R)]}{\partial R} = 0. \tag{8}$$

Clusters of critical radii are in metastable equilibrium, smaller clusters are shrinking, and larger clusters are growing. By virtue of the scaling parameter $\lambda = (4\pi\sigma/T)^{1/2} R_c$, introduced in [21], reduced radius $r = R/R_c$, and new dimensionless parameter $\gamma = 3e^2 R_c^5 / 5 T r_0^6$ we have

$$f_0(R) = f_0(R_c) \exp\left[\left(- \frac{1}{2}\gamma\delta + \frac{5}{12}\gamma + \frac{2}{3}\lambda^2 + \tau \right)(r^3 - 1) \right] \times \exp\left\{ - \lambda^2 (r^2 - 1) - 3\tau \ln r - \frac{\gamma}{4}[r^5 - 1 - \delta(r^6 - 1)] \right\}, \tag{9}$$

where

$$f_0(R_c) = I_0 \exp\left[- \frac{1}{2}\gamma\delta + \frac{5}{12}\gamma - \frac{1}{3}\lambda^2 + \tau - 3\tau \ln \frac{R_c}{r_0} + \frac{\gamma}{4}(\delta - 1) \right], \tag{10}$$

and $\delta = (\rho/\rho_L)^{1/3}$. The other parameters are the nucleon radius $r_0 = 1.17$ fm and critical exponent $\tau = 2.2$.

B. Clusterization kinetics

Under the assumption of the evaporation-condensation mechanism of the cluster evolution mentioned above, the growth of the clusters may be described by a Fokker-Planck equation [9,13]

$$\frac{\partial f}{\partial t} = - \frac{\partial J}{\partial R}, \quad J = Cf - B \frac{\partial f}{\partial R}, \tag{11}$$

where J is the flux in size space, and C and B are the size drift and size diffusion coefficients. The flux in size space, J, is absent for the equilibrium distribution given by $f_0(R)$. So, one may find the relation between the coefficients C and B

$$C=B(R)\frac{\partial}{\partial R}\left[-\frac{\Delta F(R)}{T}\right]. \tag{12}$$

The nonequilibrium, steady-state general solution of Eq. (10) corresponding to a continuous phase transition ($J=$ const) reads

$$\frac{f(R)}{f_0(R_c)}=-J\int\frac{dz}{B(z)f_0(z)}+\text{const}. \tag{13}$$

Combining this result with the boundary conditions

$$\lim_{R\to 0}\frac{f(R)}{f_0(R)}=1 \quad \text{and} \quad \lim_{R\to\infty}\frac{f(R)}{f_0(R)}=0, \tag{14}$$

we get

$$\frac{f(R)}{f_0(R)}=J\int_R^\infty\frac{dz}{B(z)f_0(z)}, \tag{15}$$

$$J^{-1}=\int_0^\infty\frac{dz}{B(z)f_0(z)}. \tag{16}$$

In terms of the critical radius R_c, reduced radius r, and dynamical prefactor $\kappa=(d/dt)\ln(R-R_c)$, introduced by Langer [22], the drift coefficient C may be rewritten in the following form [21]:

$$C=\frac{\kappa R_c}{r^2}(r-1). \tag{17}$$

Substitution of Eqs. (13) and (16) into Eq. (11) gives for the cluster size diffusion coefficient

$$B(R)=\frac{\kappa R_c^2}{r\{[(3/2)\gamma\delta r^3+3\tau](r^2+r+1)-(5/4)\gamma r^3(r+1)+2\lambda^2 r^2\}}. \tag{18}$$

Finally, the distribution function of clusters of the new phase is given by

$$f^C(R)=f_0^C(R_c)r^{-3\tau}\exp\left(\frac{\gamma\delta}{4}-\frac{\gamma}{6}-\tau+\frac{1}{3}\lambda^2\right)\exp\left[\frac{\gamma\delta}{4}r^6-\frac{\gamma}{4}r^5+\left(-\frac{\gamma\delta}{2}+\frac{5}{12}\gamma+\frac{2}{3}\lambda^2+\tau\right)r^3-\lambda^2r^2\right]\frac{\text{Int}[r,\infty]}{\text{Int}[0,\infty]},$$

$$\text{Int}[a,b]=\int_a^b z^{3\tau+1}\left[\left(\frac{3}{2}\gamma\delta z^3+3\tau\right)(z^2+z+1)-\frac{5}{4}\gamma z^3(z+1)+2\lambda^2z^2\right]$$

$$\times\exp\left[-\frac{\gamma\delta}{4}z^6+\frac{\gamma}{4}z^5-\left(-\frac{\gamma\delta}{2}+\frac{5}{12}\gamma+\frac{2}{3}\lambda^2+\tau\right)z^3+\lambda^2z^2\right]dz. \tag{19}$$

For the Fisher droplet model without Coulomb interactions Eq. (18) reduces to [10]

$$f^F(R)=f_0^F(R_c)r^{-3\tau}\exp\left[\left(\tau+\frac{2}{3}\lambda^2\right)r^3-\lambda^2r^2+\frac{\lambda^2}{3}-\tau\right]$$

$$\times\frac{\int_r^\infty z^{3\tau+1}[3\tau(z^2+z+1)+2\lambda^2z^2]\exp\{-[\tau+(2/3)\lambda^2]z^3+\lambda^2z^2\}dz}{\int_0^\infty z^{3\tau+1}[3\tau(z^2+z+1)+2\lambda^2z^2]\exp\{-[\tau+(2/3)\lambda^2]z^3+\lambda^2z^2\}dz}, \tag{20}$$

and for the classical case with bare bulk and surface terms in the cluster free energy one obtains [21]

$$f^{\text{cl}}(R)=f_0^{\text{cl}}(R_c)\exp\left(\frac{2}{3}\lambda^2r^3-\lambda^2r^2+\frac{\lambda^2}{3}\right)\frac{\int_r^\infty z^3\exp\left(-\frac{2}{3}\lambda^2z^3+\lambda^2z^2\right)dz}{\int_0^\infty z^3\exp\left(-\frac{2}{3}\lambda^2z^3+\lambda^2z^2\right)dz}. \tag{21}$$

C. Simulation results

The distribution functions given by Eqs. (18)–(20) with the critical temperature $T_c=20.69$ MeV [4] and mass of the critical cluster $A_c=16$ and $A_c=36$ are shown in Fig. 1. To calculate the surface tension we used the approximation proposed in [11]

$$\sigma(T)=\sigma_0\left(\frac{T_c^2-T^2}{T_c^2+T^2}\right)^{5/4}, \tag{22}$$

where $4\pi r_0^2\sigma_0=18$ MeV. Densities of the liquid and gaseous phases are determined as the end points of a Maxwell construction in a (p,V) plot of the nuclear equation of state [7].

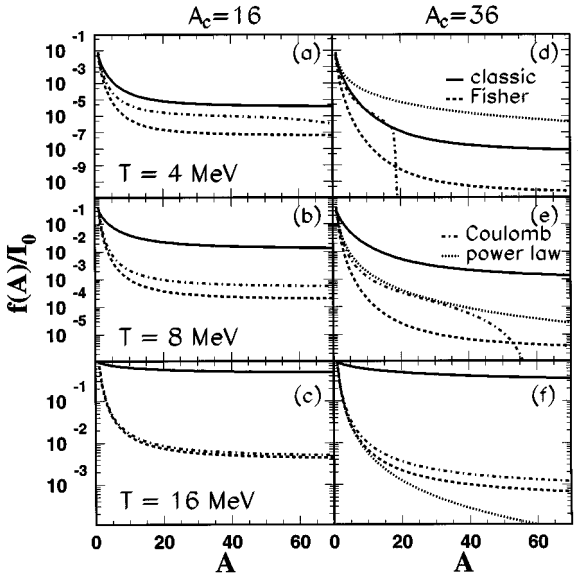

FIG. 1. The steady-state distribution functions of clusters of the new phase $f_0(R)/I_0$ given by Eq. (19) (*Coulomb*, dash-dotted line), Eq. (20) (*Fisher*, dashed line), and Eq. (21) (*classic*, full line) for three different temperatures of the system, 4, 8, and 16 MeV, respectively. The critical temperature is $T_c=20.69$ MeV, and masses of the critical nuclei are $A_c=16$ (a)–(c) and $A_c=36$ (d)–(f), correspondingly. Dotted lines in (d)–(f) represent the simple power law $A^{-2.2}$.

In the vicinity of critical point the distributions corresponding to Eqs. (18) and (19) still exhibit the power-law falloff for the fragments smaller than the fragments of critical masses, in accordance with the Fisher droplet model. The classic model with bulk and surface energy terms only predicts practically the same probabilities for the production of small and big clusters at high temperatures because of the diminishing of the surface tension. The Coulomb term leads to the shift in the tail part of the distribution function, that brings it closer to the classic distribution function. As the temperature rises, the influence of the Coulomb energy in the free energy expansion on the behavior of the distribution function seems to become negligibly weak at small values of the critical radius [Figs. 1(c) and 1(f)]. This fact may be explained by the vanishing of the difference between the baryon density inside the clusters and the average baryon density of the system. As can be easily seen from Eqs. (18)–(20), the preexponential polynomial multiplier in the integrand Int$[a,b]$ is always positive for the model with bulk, surface, and with or without curvature terms in the droplet free energy (19) and (20), but it can be negative in presence of the Coulomb interaction between the particles (18). Big values of critical radius and, therefore, γ may force the change of sign of the polynomial in the interval $0\leqslant y\leqslant 1$. In this case the fragment distribution has a characteristic convex-concave shape [Figs. 1(d) and 1(e)] that is determined by the temperature and critical radius of the system. If the critical radius would be big enough, this implies the rapid falloff in the yield of the light fragments together with the absence of the medium-size fragments, i.e., no continuous long tail in the fragment distribution [Fig. 1(d)]. Therefore, the long-range Coulomb forces may be responsible for the changing of the falloff of fragment distribution from the simple power law to more complex dependence.

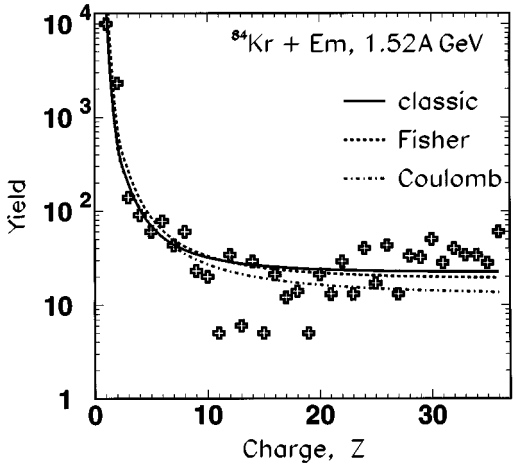

FIG. 2. The charge distribution of all fragments in ^{238}U(0.96*A* GeV) + emulsion. Data are taken from [23]. The solid, dashed, and dash-dotted lines represent the results of a fit to formulas (21) (*classic*), (20) (*Fisher*), and (18) (*Coulomb*), respectively.

III. ANALYSIS OF THE CHARGE DISTRIBUTIONS

The available experimental data on the fragment distribution are usually restricted to the light fragment production region. One of the most important predictions of the approach presented above is the existence of the nonvanishing long tail for the heavy fragment distribution together with the falloff for the yield of light fragments. Fortunately, event-by-event experiments based on the nuclear emulsion technique provide one the possibilities to identify each charged fragment. The projectile fragments can be distinguished from the target fragments also. It should be stressed here that only the fragmentation events were chosen for the further analysis.

Figure 2 shows the charge distribution of all the nonfissile fragments for ^{238}U projectile at 0.96*A* GeV induced reactions in nuclear emulsions [23]. The charge distributions of all the nonfissile fragments for the reaction ^{84}Kr+emulsion

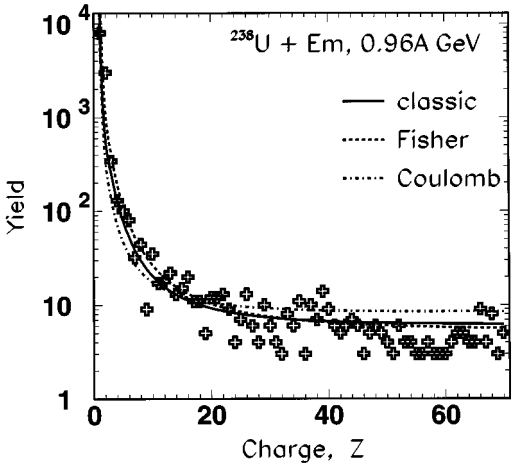

FIG. 3. The charge distribution of all fragments in ^{84}Kr(1.52*A* GeV) + emulsion. Data are taken from [24]. The sequence of the fitting curves is the same as in Fig. 2.

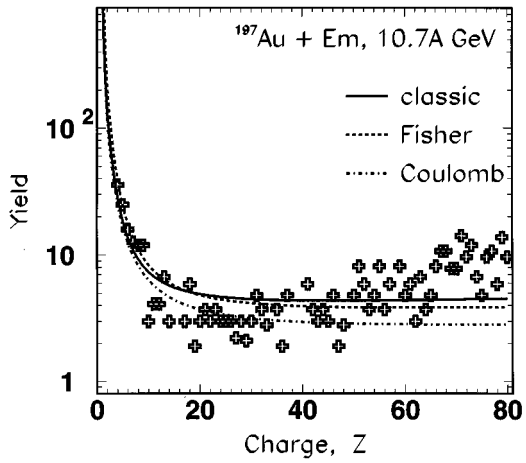

FIG. 4. The charge distribution of all projectilelike fragments in ^{197}Au(10.7A GeV) + emulsion. The number of shower particles was chosen to be less than 30 (peripheral events). Data are taken from [25]. The sequence of the fitting curves is the same as in Fig. 2.

at 1.52A GeV [24], and ^{197}Au+emulsion at 10.7A GeV (peripheral events only) [25] are shown in Figs. 3 and 4, respectively. Curves plotted onto the experimental data are the results of the fit to formulas (18)–(20). Parameters of the fit are listed in Table I. The absolute normalization $f_0(R_c)$ is always taken as a free parameter. Although the curves corresponding to the fits coincide within a few percent of accuracy, the temperatures and masses of the critical fragments are different for the different approximations of a cluster free energy. It is easy to see that the classical model predicts the lowest temperature for the splitting system among the three models. The systems should have different temperatures of disintegration, because the temperature of the disassembled fireball depends on the excitation energy of the system. A fireball with higher initial excitation energy possesses the higher temperature when passing the disintegration point, and fit to all three models demonstrates this tendency.

The possible rise in the yield of heavy fragments may be explained by the coalescence of two or more clusters, that is not included in our model. On the other hand, the relative enhancement of the heavy fragments may be explained by admixture of the remnants of primordial nuclei broken after the peripheral collisions. More data on the central collisions of heavy ions of about the same sizes are needed to shed light on this extremely interesting problem. These data are very important also for the comparison between different theoretical models [26].

The reason why the experimental data can be described equally with the three different approximations is the following. The radius of the critical nucleus and the temperature of the system are correlated. The closer the temperature to the critical one, the larger should be the critical radius, as it can be seen from Table I. But, since we do not know the vapor saturation in the system, we must take the critical size as a free parameter. In contrast to the approach given by Eq. (1), that contains bulk and surface energies as fitting parameters, the approach proposed has also two fitting parameters, T and A_c. From Fig. 1 it follows that the shapes of the distributions given by Eqs. (18)–(20) are very similar in the region far

TABLE I. The results of the fit of fragment charge distributions to expressions (19) (Coulomb), (20) (Fisher), and (21) (classic). Of each pair of numbers, the upper one denotes the temperature and the lower one denotes the charge of the critical nucleus.

Approximation		^{84}Kr+Em 1.52A GeV	^{238}U+Em 0.96A GeV	^{197}Au+Em 10.7A GeV	^{197}Au+X 0.6A GeV
Classic	T	3.1±0.2	7.4±0.1	4.0±1.4	4.7±0.1
	Z_c	5.2±0.4	13.9±0.1	6.5±1.2	9.2±0.2
Fisher	T	6.6±0.2	11.5±0.2	8.9±1.8	9.6±0.2
	Z_c	6.8±0.4	15.7±1.6	8.8±0.8	12.4±0.3
Coulomb	T	8.1±0.6	7.6±0.4	9.1±0.8	6.65±0.4
	Z_c	9.8±0.7	9.6±0.3	10.9±1.0	8.7±0.4

from the critical temperature. Therefore, to distinguish between the approximations one has to know either the disassembly temperature of the system or the mass of the critical nucleus. Unfortunately, both these problems cannot be solved unambiguously. First of all, it is not clear how to determine the critical nuclei experimentally. Then, the breakup temperature, that can be estimated from the analysis of data in a different way, is model dependent.

For instance, if one assumes that local thermal and chemical equilibrium is reached, the temperature of the system may be obtained via the double ratios of light isotope pairs varying by one neutron each [27]. The ALADIN Collaboration reported recently [28] results on their studying of fragment distributions coming from Au+Au collisions at 600A MeV. A temperature scale was derived from observed yield ratios of He and Li isotopes, and the transition isotopic temperature, T_{HeLi}, was found to be about 5±0.2 MeV. Combined charge spectrum measured by the ALADIN detector systems for the reactions with gold projectiles [29] is shown in Fig. 5. It looks very similar to the spectra shown in Figs. 2–4. Results of the fit to formulas (18)–(20) are listed in Table I. The corresponding curves are plotted onto the experimental data also. Although all three models predict prac-

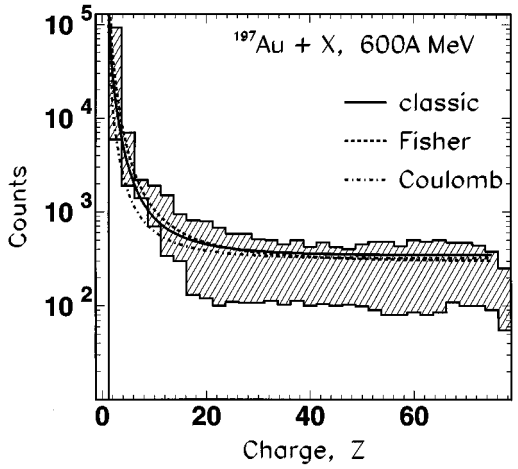

FIG. 5. Combined charge spectrum measured with the ALADIN tracking detectors for reactions with ^{197}Au projectiles at 0.6A GeV. Data are taken from [29] (hatched area). The sequence of the fitting curves is the same as in Fig. 2.

tically the same yield ratios for the light isotopes, the temperatures obtained by fit to Eqs. (18)–(20) differ considerably from the temperature derived from the caloric curve of nuclei. This is a consequence of the nonequilibrium process of a first-order phase transition in nuclear matter which was chosen as an underlying mechanism for the condensation of hot nucleonic gas. One of the possible ways to verify the validity of the approach proposed is to search for the characteristic convex-concave shape of the fragment yield shown in Figs. 1(d) and 1(e). The experiment may be performed with the heavy nuclei, like gold or lead, at not very high energies, say, between 30 and 50 MeV per nucleon of the projectile for the central collisions.

IV. CONCLUSIONS

Under the assumption of a first-order phase transition in the thermalized system of initially unbound nucleons, a new method for calculating fragment mass distributions has been proposed. This approach is based on the steady-state solution of Fokker-Planck equation describing the evolution of fragments of the new phase. To calculate the cluster free energy the Myers-Swiatecki formula generalized to nonzero temperatures is used.

It is shown that the inclusion of the Coulomb energy in the form provided by the Wigner-Seitz approximation does not affect qualitatively the behavior of the fragment mass distributions in the vicinity of critical point. At lower temperatures the Coulomb interaction between particles may lead to the transformation of the shape of fragment distribution from power-law to the more complex convex-concave shape. This prediction may be tested in an experiment with the heavy-ion central collisions at not very high excitation energies.

We have shown that the fragment charge (mass) distributions may contain important information about the underlying dynamics of the clusterization process in hot nuclear matter. Although the expressions derived fit to experimental data quite nicely, more data on the yield of nuclear fragments coming from the 4π-geometry detectors are needed to make these formulas useful for calculation of the fragment distributions.

ACKNOWLEDGMENTS

This work was supported by the Norwegian Research Council (NFR) under Contract No. 100132/432. We would like to thank J. P. Bondorf, L. P. Csernai, B. Jakobsson, I. N. Mishustin, and Yu. Murin for the helpful suggestions and comments. We are indebted to the Department of Physics, University of Bergen for the warm and kind hospitality.

[1] J. E. Finn, S. Agarwal, A. Bujak, J. Chuang, L. J. Gutay, A. S. Hirsch, R. W. Minich, N. T. Porile, R. P. Scharenberg, B. C. Stringfellow, and F. Turkot, Phys. Rev. Lett. **49**, 1321 (1982); R. W. Minich, S. Agarwal, A. Bujak, J. Chuang, J. E. Finn, L. J. Gutay, A. S. Hirsch, N. T. Porile, R. P. Scharenberg, B. C. Stringfellow, and F. Turkot, Phys. Lett. **118B**, 458 (1982).
[2] M. E. Fisher, Physics **3**, 255 (1967).
[3] H. R. Jaqaman, A. Z. Mekjian, and L. Zamick, Phys. Rev. C **29**, 2067 (1984).
[4] A. L. Goodman, J. I. Kapusta, and A. Z. Mekjian, Phys. Rev. C **30**, 851 (1984).
[5] A. D. Panagiotou, M. W. Curtin, H. Toki, D. K. Scott, and P. J. Siemens, Phys. Rev. Lett. **52**, 496 (1984); A. D. Panagiotou, M. W. Curtin, and D. K. Scott, Phys. Rev. C **31**, 55 (1985).
[6] L. P. Csernai and J. I. Kapusta, Phys. Rep. **131**, 223 (1986).
[7] A. R. DeAngelis and A. Z. Mekjian, Phys. Rev. C **40**, 105 (1989).
[8] M. L. Gilkes *et al.*, Phys. Rev. Lett. **73**, 1590 (1994).
[9] E. M. Lifshitz and L. P. Pitaevskii, *Physical Kinetics* (Pergamon, Oxford, 1981), Chap. 12.
[10] E. E. Zabrodin, Phys. Rev. C **52**, 2608 (1995).
[11] J. P. Bondorf, A. S. Botvina, A. S. Iljinov, I. N. Mishustin, and K. Sneppen, Phys. Rep. **257**, 133 (1995); J. P. Bondorf, R. Donangelo, I. N. Mishustin, C. J. Pethick, H. Schulz, and K. Sneppen, Nucl. Phys. **A443**, 321 (1985).
[12] R. Becker and W. Döring, Ann. Phys. (Leipzig) **24**, 719 (1935).
[13] Ya. B. Zeldovich, Acta Physicochim. (USSR) **18**, 1 (1943).
[14] F. P. Kelly, *Reversibility and Stochastic Networks* (Wiley, New York, 1979).
[15] K. C. Chase and A. Z. Mekjian, Phys. Rev. C **49**, 2164 (1994).
[16] D. H. E. Gross, Prog. Part. Nucl. Phys. **30**, 155 (1993); Nucl. Phys. **A553**, 175c (1993).
[17] R. J. Charity *et al.*, Nucl. Phys. **A483**, 371 (1988).
[18] J. Randrup *et al.*, Prog. Part. Nucl. Phys. **30**, 117 (1993).
[19] W. Myers and V. Swiatecki, Ann. Phys. (N.Y.) **55**, 395 (1969).
[20] P. Marmier and E. Sheldon, *Physics of Nuclei and Particles* (Academic Press, London, 1969).
[21] L. V. Bravina and E. E. Zabrodin, Phys. Lett. A **202**, 61 (1995).
[22] J. S. Langer, Ann. Phys. (N.Y.) **54**, 258 (1969).
[23] P. L. Jain, G. Singh, and M. S. El-Nagdy, Phys. Rev. Lett. **68**, 1656 (1992).
[24] P. L. Jain and G. Singh, Phys. Rev. C **46**, R10 (1992).
[25] B. Jakobsson, in *Multiparticle Correlations and Nuclear Reactions*, edited by J. Aichelin and D. Ardouin (World Scientific, Singapore, 1995), p. 373.
[26] L. V. Bravina and E. E. Zabrodin, Phys. Rev. C **54**, R464 (1996).
[27] S. Albergo, S. Costa, E. Costanzo, and A. Rubbino, Nuovo Cimento A **89**, 1 (1985).
[28] J. Pochodzalla *et al.*, Phys. Rev. Lett. **75**, 1040 (1995).
[29] W. F. J. Müller *et al.*, Report GSI 03-95, 1995.